www.czasopisma.pan.pl PAN POLSKA AKADEMIA NAUK www.journals.pan.pl

POLISH POLAR RESEARCH
vol. 31, no. 1, pp. 17–32, 2010 doi: 10.4202/ppres.2010.02

Spatial information on total solar radiation: Application and evaluation of the r.sun model for the Wedel Jarlsberg Land, Svalbard

Maciej KRYZA[1], Mariusz SZYMANOWSKI[2], Krzysztof MIGAŁA[1] and Małgorzata PIETRAS[1]

[1] *Uniwersytet Wrocławski, Instytut Geografii i Rozwoju Regionalnego, Zakład Klimatologii i Ochrony Atmosfery, Kosiby 6/8, 51-670 Wrocław, Poland*

[2] *Uniwersytet Wrocławski, Instytut Geografii i Rozwoju Regionalnego, Zakład Kartografii, pl. Uniwersytecki 1, 50-137 Wrocław, Poland*

<kryzam@meteo.uni.wroc.pl> <szymanma@meteo.uni.wroc.pl> <migalak@meteo.uni.wroc.pl> <pietras@meteo.uni.wroc.pl>

Abstract: The results of the application and evaluation of the r.sun model for calculation of the total solar radiation for the Wedel Jarlsberg Land (SW Spitsbergen) are presented. Linke Turbidity Factor (LTF), which is the obligatory parameter for direct and diffused radiation calculations with the r.sun model, is derived here with the empirical formula and meteorological measurements. Few different approaches for calculation of LTF are presented and tested. The r.sun model results, calculated with these various LTF, are evaluated through comparison with total solar radiation measurements gathered at Polish Polar Station. The r.sun model is found to be in good agreement with the measurements for clear sky conditions, with the explained variance (R^2) close to 0.9. Overall, the model slightly underestimates the measured total radiation. Reasonable results were calculated for the cloudiness condition up to 2 octas, and for these r.sun model can be considered as a reliable and flexible tool providing spatial data on solar radiation for the study area.

Key words: Arctic, Spitsbergen, solar radiation, r.sun, Linke Turbidity Factor, GIS GRASS.

Introduction

Deglaciation of the Svalbard area has been observed since the beginning of the 20th century and it is attributed to the contemporary global scale climate changes. The process modifies the proportions of the surface energy balance, dynamics of the hydroglaciological processes and microclimatological conditions. According to Jania (1997), evolution of the Svalbard glaciers should be understood as the changes

in their hydrological and thermal structure, caused by the climate changes. The glaciers ablation is also an important factor in energy exchange between the atmosphere and land ice masses. The dynamics of ablation closely reflects climate changes and is important for the estimation of the outflow of meltwater, which, having penetrated a glacier to bedrock, stimulates its velocity by increasing basal sliding (Zwally *et al.* 2002; Vieli *et al.* 2004; Van der Wal *et al.* 2008). Surface melting is the main source of liquid water in glaciers. Melting intensity depends, among others, on the solar radiation amount reaching the earth (glacier) surface, which is a key component of the energy budget of the glacier surface. This is why the spatial information on solar radiation reaching the glacier surface is a first step in assessing the amount of meltwater intruding the glacier and influencing its hydrological structure. It is also a key input information for various modelling studies (Hodgkins 2001; Pohl *et al.* 2006).

Solar radiation reaching the Earth's surface is a result of complex interactions of energy exchange between the atmosphere and surface. Spatio-temporal modelling of the incoming solar energy for the Arctic areas is even more challenging because of the low solar elevations, which make terrain shadowing a key factor influencing the results. The other issue is related with atmospheric aerosol properties which change seasonally and have large influence on the solar radiation attenuation (Lund Myhre *et al.* 2007; Yamanouchi *et al.* 2005; Toledano *et al.* 2006; Krzyścin and Sobolewski 2001).

Spatial variation of solar radiation in the complex terrain can be assessed with the solar radiation models integrated with the Geographical Information Systems (GIS). Main input data for such models are usually digital elevation model (DEM) and its derivatives: slope, aspect and terrain shadowing. Solar models available through the GIS have been developed since 1990s. The first models were based on simple empirical formulas describing attenuation of the solar radiation in the atmosphere, e.g. SolarFlux for ArcInfo (Hetrick *et al.* 1993; Dubayah and Rich 1995), Solei for Idrisi (Miklánek 1993) and Genasys (Kumar *et al.* 1997). More advanced solutions for solar radiation estimation are implemented in Solar Analyst model, which is an extension of ESRI ArcGIS (Fu and Rich 2000) and the SRAD model (McKenney *et al.* 1999). Despite being developed and suitable for fine-scale analysis, the models mentioned come with a number of limitations related mainly with the diffused solar radiation computation and the limited, due to technical reasons, applicability for the large areas (Šuri and Hofierka 2004). The r.sun model, which is used here and available through the open source GIS GRASS environment (GRASS DEVELOPMENT TEAM 2006), is free from the mentioned drawbacks and can be efficiently used for both large areas and high spatial resolution data. The models not related with any specific GIS system are also developed to study specific issues related with solar radiation in complex terrain, *e.g.* Hock and Holmgren (2005) and Klok and Oerlemans (2002).

Because the sparse radiation and meteorological measurements are the common case for the Arctic areas, the model simplicity, in terms of atmospheric pro-

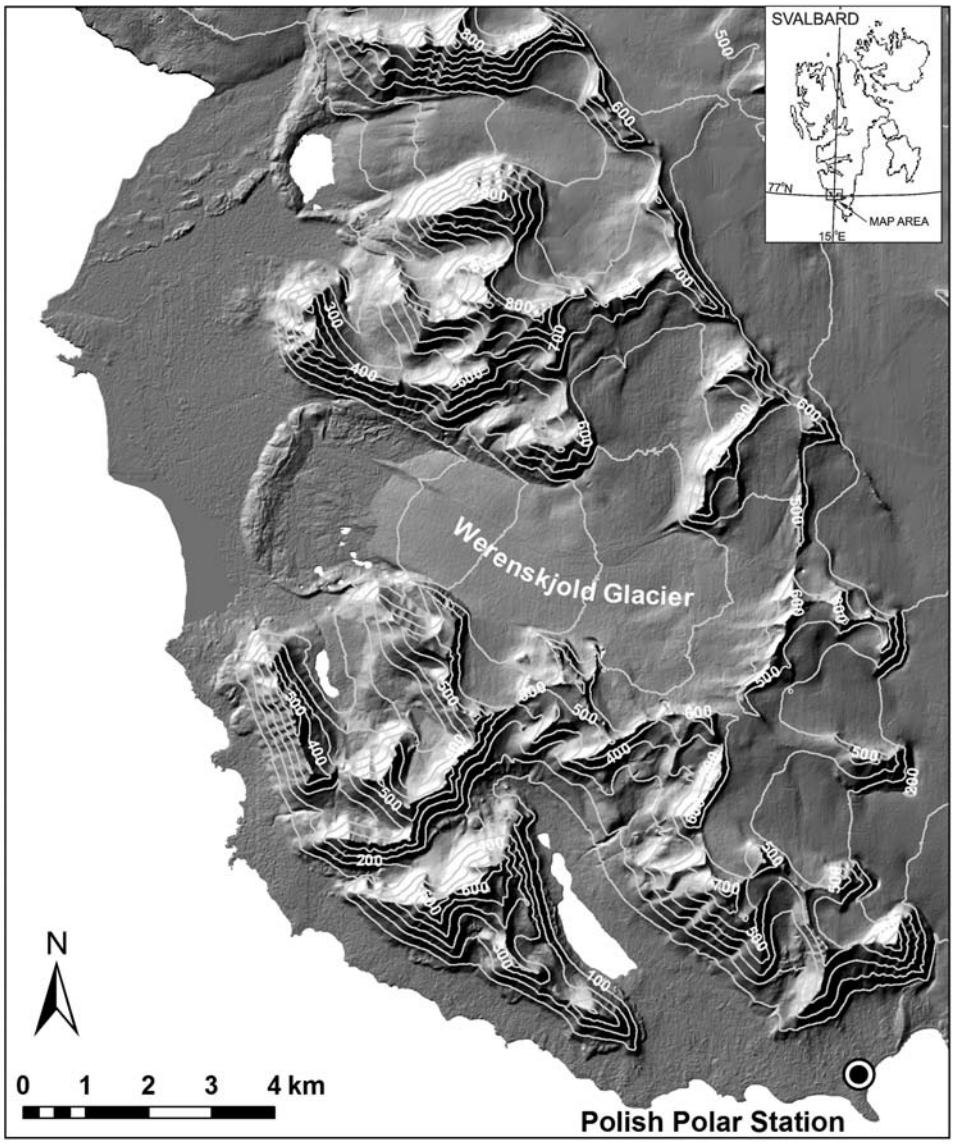

Fig. 1. Digital elevation model for the study area.

cesses parameterization, is in this case a virtue. Low number of model parameters, if complemented with good model performance, will assure wide applicability of the model and its results. The main aim of the paper is the derivation of the spatial data on incoming total (direct+difuse) solar radiation with the r.sun model for the area of Wedel Jarlsberg Land (SW Spitsbergen) with high spatial and temporal resoultion. The r.sun model is described and the main equations are presented. The methods for calculation of the key model parameters, including Linke Turbidity

Factor, are discussed. The results are evaluated by comparison with the measurements collected at the Polish Polar Station (PPS). Finally, the spatial patterns of r.sun modelled solar radiation are presented for a selected day with strong Arctic haze phenomena (2 May 2006), to show the impact of model parameterization on the final results.

Methods and data

Study area. — The study area is the surroundings of the Werenskjold Glacier in the SW Spitsbergen (Wedel Jarlsberg Land), in the vicinity of the PPS in the Hornsund Fjord (Fig. 1). The whole area covers 288 km^2; the elevation changes from the sea level to 948 m a.s.l. and the steepest slopes reach 68 degrees.

Model description. — Conceptually the r.sun model is based on the equations published in the European Solar Radiation Atlas (Scharmer and Greif 2000; Page *et al.* 2001) and on previous work by Hofierka (1997). The model is designed to calculate the irradiance [W m^{-2}] and irradiation [W h m^{-2}] for both clear-sky and overcast conditions and works in two modes. In the first mode, raster maps of instantaneous direct (IB), diffuse (ID) and reflected solar irradiance [W m^{-2}], together with the solar incident angle [degrees] can be calculated for a given day and time. In the second mode the spatial patterns of daily sums of solar irradiation [W h m^{-2}] and duration of the direct irradiation [minutes] are computed. The model requires only a few mandatory input parameters: elevation above the sea level; slope and aspect of the terrain; local solar time (for mode 1); and a day number (for both modes). The user may also change the default setting of other parameters, including atmospheric turbidity factor, ground albedo and real sky radiation coefficients separately for direct and diffuse components. Spatially distributed parameters can be set as raster maps. Optionally, the model accounts for obstructions of the sky by local terrain features from the DEM. For this study, the model is always run with the respect of the terrain shadowing which is of special importance for the Svalbard area due to low solar elevation angles and terrain complexity. The astronomical parameters, such as solar declination, are computed internally by the model.

The main model equations used for calculations of direct and diffused solar radiation reaching the surface are summarized below after Šuri and Hofierka (2004). The starting point in solar radiation calculation is the solar constant (I_o), equal to 1367 W m^{-2}. The model considers the eccentricity of the Earth orbit with the correction factor e applied in calculation of the extraterrestrial irradiance G_o normal to the solar beam:

$$G_o = I_o e$$

where: $e = 1 + 0.03344 \cos(j - 0.048869)$ and day angle j is in radians.

www.czasopisma.pan.pl PAN POLSKA AKADEMIA NAUK www.journals.pan.pl

The attenuation of the direct irradiance normal to the solar beam B_{oc} is calculated with the following equation:

$$B_{oc} = G_o \exp(-0.8662 \times LTF \times m \times \delta_R(m))$$

where: LTF is Linke Turbidity Factor, m is relative optical air mass and δ_R is the Rayleigh optical thickness at air mass m. More details on LTF are given in Model parameterization section.

The direct irradiance on a horizontal surface B_{hc} is calculated as:

$$B_{hc} = B_{os} \sin(h_o)$$

where h_o is the solar altitude.

Finally, the direct irradiance on an inclined surface B_{ic} is given as:

$$B_{ic} = B_{hc} \sin(d_{\exp}) / \sin(h_o)$$

where $d_{\exp}$ is the solar incidence angle measured between the Sun and inclined surface.

The modelling of the diffuse component for a horizontal surface [W m^{-2}] for a clear sky condition D_{hc} is calculated as a product of the G_o and a diffuse transmission function T_n dependent only on the LTF and $F_d(h_o)$ is the solar altitude function, which also depends on LTF:

$$D_{hc} = G_o T_n (LTF) F_d(h_o)$$

The diffuse irradiance on inclined surface D_{ic} is calculated with two equations, depending on weather the raster is a sunlit or shadowed surface:

Sunlit surface: $D_{ic} = D_{hc}(F(g_N)(1 - K_b) + K_b \sin(d_{\exp})) / \sin(h_o)$

Shadowed surface: $D_{ic} = D_{hc}F(g_N)$

where $F(g_N)$ is a function accounting for the diffuse sky irradiance and K_b is a proportion between direct irradiance and extraterrestrial solar irradiance on horizontal surface. The Linke turbidity factor is a key model parameter, as atmospheric turbidity increases the diffuse radiation and decreases the direct radiation. LTF parameterization used in this study is discussed in the next sections.

The estimation of the clear-sky ground reflected irradiance for inclined surfaces and computation of overcast irradiation have not been performed in this study. The detailed description of the procedure can be found in Hofierka and Šuri (2002) or Šuri and Hofierka (2004).

The r.sun model can be used, as mentioned above, to calculate instantaneous or daily radiation. The model output may be aggregated to other time spans. This can be done effectively, for example, with Linux shell script capabilities. In this paper, spatial patterns of daily total (direct+diffused) radiation are presented, whereas the model validation is based on measured instantaneous data.

Model parameterization. — The main parameter influencing the solar radiation estimates calculated with the r.sun model is LTF. Detailed description of LTF

was given by Vida *et al.* (1999) and Louche *et al.* (1986) and only the major concepts will be given here for clarity.

LTF is the ratio of the broad band extinction coefficient at unit air mass (δ) to Rayleigh's optical thickenss (δ_R). δ_R is the optical thickness of a pure Rayleight scattering atmosphere, per unit area mass along a specified path length. LTF can be interpreted as the number of clean dry atmospheres that would be necessary to produce the same attenuation of the extraterrestrial radiation that is produced by the real atmosphere. According to this definition, LTF must be greater than 1 and it is a single index combining the influence of precipitable water vapour content (PWC) and the attenuation due to aerosols.

In this paper, LTF was approximated with the empirical formula proposed by Dogniaux (1984), given here after Vida *et al.* (1999):

$$LTF = \left(\frac{85 + \gamma}{39.5 \exp(-PWC) + 47.4} + 0.1 \right) (16 + 0.22 PWC) AOT$$

where:
γ is the solar elevation angle in degrees,
PWC is the precipitable water vapour content in cm,
AOT is the aerosol optical thickness (dimensionless) expressing the aerosol content of the atmosphere in the zenith direction. It is defined as the aerosol optical thickness corresponding to a wavelength of 1 μm (Utrillas *et al.* 2000).

The formula proposed by Dogniaux (1984) was found to be in good agreement with measurements by Jacovides (1997). The LTF is assumed here to be constant over the study area. According to the formula, LTF depends on the solar elevation angle, which varies during the day. LTF was therefore calculated for each hour of the April–September period for the years 2005 and 2006. Information on PWC for this period is available from aerological soundings from nearby Bjørnøya meteorological station (74°31'N, 19°10'E). The Bjørnøya station is used here instead of Ny-Ålesund due to data completeness. The soundings are available twice a day at 00 and 12 UTM. Linear interpolation is performed to calculate the PWC values for the transitional hours.

Aerosol optical thickness at 1020 nm is measured at the PPS in Hornsund Fjord (SW Spitsbergen). The data are available through AERONET (Aerosol Robotic Network) project database (http://aeronet.gsfc.nasa.gov) and are used here for LTF calculation (Fig. 2). The measured AOT varies significantly within the study period (Fig. 2). In general, AOT values are higher for April and May than for summer and autumn months, with measured maximum exceeding 0.16 in the beginning of May 2006. Day to day variations also seem to be larger during spring time. Nine out of ten smallest values for the study period were measured during late August and September 2006, and are all below 0.02. High AOT values during April and May are commonly reported for the Arctic area (Lund Myhre *et al.* 2007) and can be attributed to

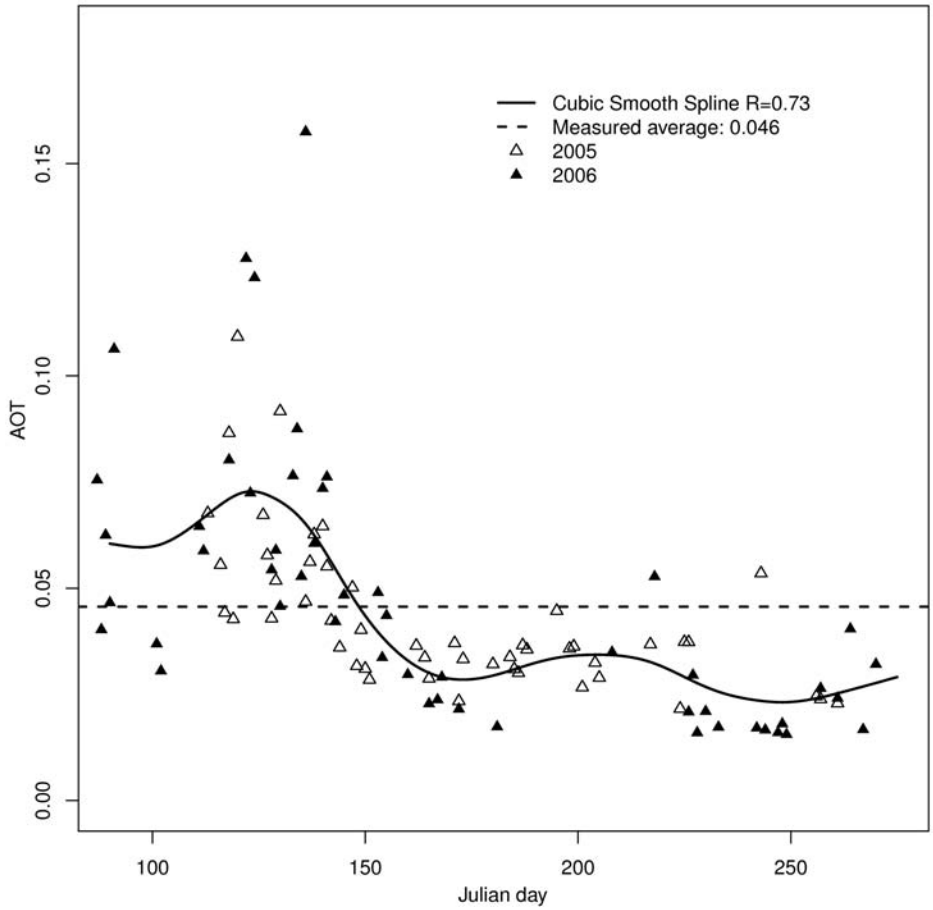

Fig. 2. Aerosol optical thickness (AOT) for the study period, Polish Polar Station, Hornsund.

the phenomena known as the Arctic haze, which was discussed *e.g.* by Herber *et al.* (2002) and Yamanouchi *et al.* (2005).

Two approaches are used in this study for the LTF computation with Dogniaux formula, varying in terms of AOT parameter specification. First, AOT turbidity coefficient is kept constant during the year (CA for Constant AOT). The mean value calculated from the data available for the period of interest is 0.047 (standard deviation 0.026) and is used for LTF calculation. This is also close to the value of 0.05 suggested by Vida *et al.* (1999) for rural areas.

For the second approach, the cubic smooth spline (CSS) function is fitted into the available AOT measurements to describe the seasonal variation of aerosol optical thickness (SA for Seasonal AOT; Fig 2). The CSS function was able to cover the general pattern of increased spring aerosol concentrations, reflected in measurements and reported by Lund Myhre *et al.* (2007) and Yamanouchi *et al.* (2005) as the Arctic haze phenomena. There is reasonably good agreement between the

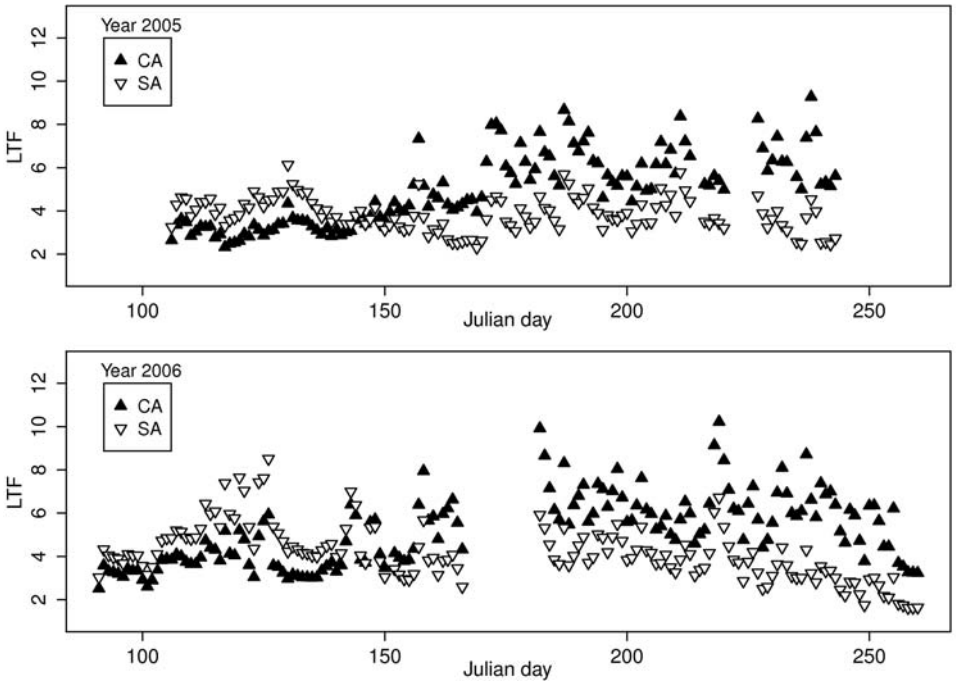

Fig. 3. Daily average Linke Turbidity Factor (LTF) for constant (CA) and modelled aerosol optical thickness (SA).

measured and modelled CSS values, with the correlation coefficient over 0.7. The other tested methods, based on polynomial and local polynomial regression, gave worse results in terms of the correlation coefficient.

As mentioned above, the aim for the SA approach is to cover the seasonal variability of the AOT coefficient. The large AOT values, measured in spring 2005 and, especially at the beginning of May 2006, are not covered with this simple CSS function fit. However, as the paper is mainly focused on the methodological aspect of the spatial modelling of incoming solar radiation, the authors found it interesting to compare the results for CA and SA approaches and their influence on the final results calculated with the r.sun model.

For the period of interest, LTF varies from near 2 at the autumn of 2005 and 2006, to over 8 in spring 2006 for the SA approach (Fig. 3). In case of CA, the largest values are calculated for summer, as a result of high solar elevation angle and PWC. In general, LTF values calculated for SA approach are larger for the spring months as a result of the CSS function approximation. Day to day variation is higher for CA, as a consequence of varying PWC.

Dogniaux formula (Dogniaux 1984), used here for LTF parameterization, is an indirect approach for turbidity calculation. Due to the lack of data, it was not possible to validate the results with direct measurements.

www.czasopisma.pan.pl PAN POLSKA AKADEMIA NAUK www.journals.pan.pl

GIS data. — Digital elevation model and spatial information on slope inclination and aspect are obligatory input data for solar radiation modelling with the r.sun model. Here, 10 m × 10 m DEM model is used, based on the source data for the orthophotomap (1:25000) "Werenskioldbreen and surrounding areas" (© Norsk Polarinstitutt and University of Silesia, Poland; Fig. 1). Slope and aspect have been calculated from DEM using r.slope.aspect module available through GIS GRASS system (GRASS Development Team 2006).

Model validation. — Total radiation measurements and cloud amount (in octas) data are available from the PPS (77°00'N, 15°33'E; Fig. 1). The radiation measurements are preformed with the 5 minutes interval, but the information on the cloudiness is available every 3 hours. For model evaluation, only those radiation measurements were used for which data on cloudiness are available. In case of cloudiness amount, there is only information on sky coverage for both low and middle level clouds (CL). Therefore, the clear sky conditions were defined on the basis of CL, and the total radiation for the CL < 2 cases is used for the model evaluation. Total number of radiation and cloudiness cases available for the April–September period for the years 2005 and 2006 is 2440.

The r.sun model calculates direct and diffuse solar radiation separately. These were added to calculate total solar radiation and compared with the instantaneous total solar radiation measured at the PPS. The results of model – measurements intercomparison are presented on the scatterplot for the clear sky conditions (CL < 2). For different cloudiness conditions, various error statistics are calculated to evaluate the model performance. The error metrics, which are used in this paper, are summarized in Table 1 after Yu *et al.* (2006).

Mean bias (MB) is used here as a general measure of under- or overestimation of the model. Mean absolute gross error (MAGE) and root mean square error

Table 1

Quantitative metrices used in model validation (N – total number of pairs, M_i – modelled solar radiation, O_i – measured solar radiation)

Metrices	Mathematical expression
Mean Bias	$MB = \frac{1}{N}\sum_i (M_i - O_i)$
Mean Absolute Gross Error	$MAGE = \frac{1}{N}\sum_i \lvert M_i - O_i \rvert$
Root Mean Squared Error	$RMSE = \sqrt{\frac{1}{N}\sum_i (M_i - O_i)^2}$
Normalized Mean Bias	$NMB = \frac{\sum (M_i - O_i)}{\sum O_i}$
Normalized Mean Absolute Error	$NMAE = \frac{\sum \lvert M_i - O_i \rvert}{\sum O_i}$

(RMSE) are commonly used for mean error description and are used here. Two measures of relative (normalized) difference, normalized mean bias (NMB) and normalized mean absolute error (NMAE) are useful in comparing the performance of the model for different cloudiness conditions or for the month to month intercomparison, when absolute radiation values may vary significantly due to the changes in solar elevation angle, cloudiness or both. It should be mentioned that normalized error statistics are prone to outliers, *i.e.* small number of relatively large errors may influence the error metrices significantly (Yu *et al.* 2006).

The main aim of the paper is the application and evaluation of the model for the clear sky conditions, but it seems also interesting how the model error changes with the increasing cloudiness. This can give an insight on the model applicability and answer the question if there is a threshold value of cloudiness for which the modelled results can be treated as a reasonable approximation of the real solar radiation. Therefore, the normalized error statistics are calculated for different cloudiness amounts. The error metrices are also calculated for the separate months for the years 2005 and 2006. This is performed to assess the role of the assumed constant AOT, and the NMB statistics is used to address the issue. Spring months are expected to give larger errors in case of CA approach, due to considerably higher aerosol optical thickness and Arctic haze.

Results and discussion

Spatial pattern of the modelled daily solar radiation is presented for 02 May 2006. For this day, extremely high AOT values were measured at PPS, reaching 0.12. The episode, named Arctic smoke (Lund Myhre *et al.* 2007; Stohl *et al.* 2007), was caused by the specific circulation condition, favourable for air pollution transport from Central and Eastern Europe.

For comparison, spatial patterns of total solar radiation are presented for CA (AOT equal to 0.047), SA (AOT equal to 0.07 for this day, approximated with CSS) and LTF calculated for measured AOT (0.12; Fig. 4). It should be mentioned that the cloudiness for selected day was high; therefore the comparison is strictly theoretical with the aim to assess the AOT variability on the modelled spatial patterns of total radiation.

The aerosol optical thickness has large impact on absolute values of modelled total radiation. The influence is different on direct and diffuse component. Total radiation modelled on southerly exposed slopes decreases with increasing LTF (due to the increasing AOT), as a result of overall attenuation of IB. Direct radiation is a main component of total flux for south facing slopes. The differences between CA and real LTF can reach 80 W m^{-2}. In case of northern slopes, there is an increase in total radiation with increasing LTF due the large contribution of diffuse component.

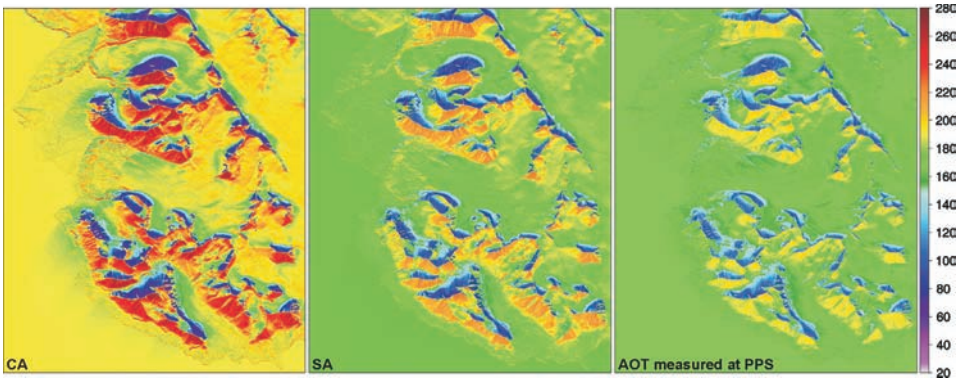

Fig. 4. Modelled incoming total solar radiation for constant (CA), modelled (SA) and measured aerosol optical thickness. All maps are for 2 May 2006.

The modelled total radiation (direct + diffuse) is in close agreement with the measurements performed at the Polish Polar Station, with the coefficient of determination close to 0.9 (Fig. 5) for the clear sky condition (CL < 2) in both CA and SA. The R^2 calculated for the SA is slightly lower than for CA. The scattering for the SA approach seems to be higher for the measured values in the range from 300 to 400 W m^{-2}. For both SA and CA, there are a few situations for which the modelled values are above 2:1 line or below 1:2, which are thresholds commonly considered as a large over or underestimation.

The model tends to underpredict the total radiation for the clear sky conditions for SA and CA. This is suggested by the regression slope and intercept, and is supported by MB equal to -12.5 and -9.9 for CA and SA, respectively, and the differences are statistically significant (Table 2). Noticeably, SA gives MB that is closer

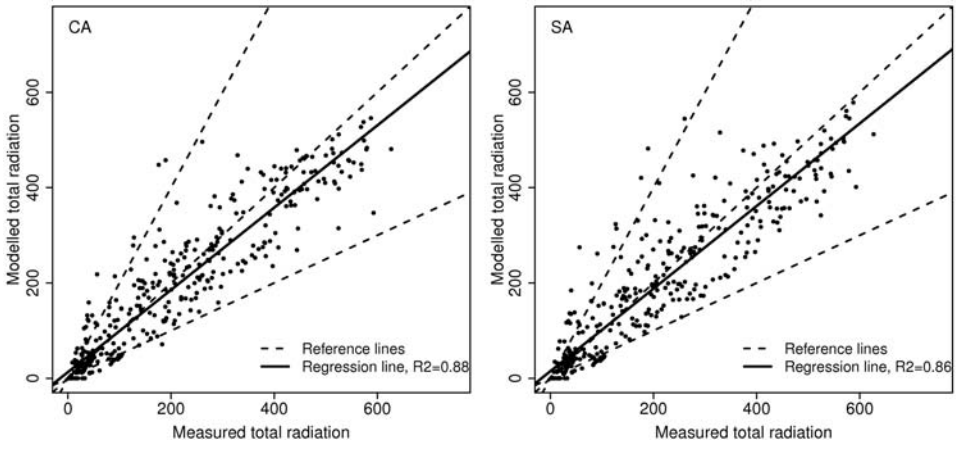

Fig. 5. Modelled *vs* measured total solar radiation (Polish Polar Station, Wm^{-2}) for cloudiness < 2. 1:1, 2:1 and 1:2 lines (dashed) and regression line (solid) are given for clarity.

Table 2

Error statistics for CA and SA approach under clear sky conditions (CL < 2; see Table 1 for abbreviations)

	MB	MAGE	RMSE	NMB	NMAE
CA	-12.47	43.63	61.39	-0.07	0.24
SA	-9.90	45.59	65.26	-0.05	0.25

to zero than MB for CA, despite the smaller R^2. The underestimation can be attributed to three different reasons:

1. Wrong aerosol optical thickness parameterization. As shown in Fig. 2, AOT may differ considerably from day to day, and both CA and SA approaches are too simple to fully cover this variability.

2. Information on cloudiness is given for low and medium level together. Data on high level cirrus clouds are not available, therefore general assumption for model validation is that no low and medium level cloudiness means also no cirrus cloud, which is not always the case.

3. Uncertainties related with the LTF approximation.

Error statistics for CA and SA are summarized in Table 2. All metrices, excluding MB and NMB suggest that the simulation with constant AOT coefficient used for LTF calculation resulted in overall better approximation of the real solar radiation conditions.

Constant AOT simplification is expected to cause an increase of NMB or NMAE for springtime due to the underestimation of the aerosol effect on the solar radiation, resulting in overestimation of the modelled solar radiation. This is not supported by the simulation results for year 2005 and 2006 (Fig. 6). In fact, the model underestimates the solar radiation, and the underestimation is larger for SA

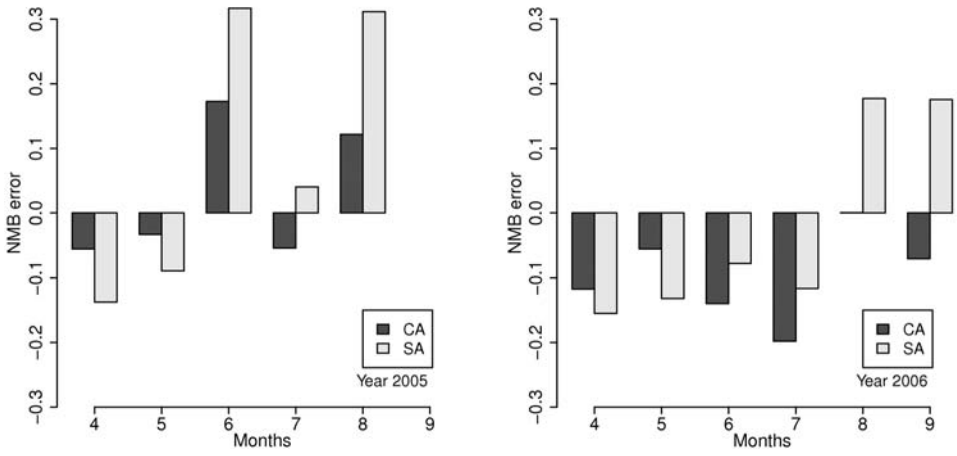

Fig. 6. Monthly Normalized Mean Bias (NMB) for NH < 2.

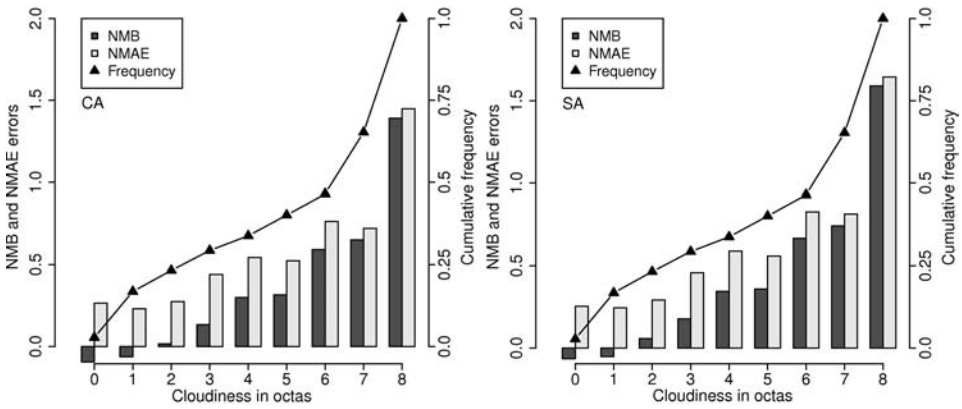

Fig. 7. Normalized Mean Bias (NMB) and Normalized Mean Absolute Error (NMAE) for different low and middle level cloudiness conditions (in octas, cumulative frequency).

due to higher AOT values calculated with CSS function. For 2005, the model overestimates total radiation values for June and August, while in 2006, the model is higher than measurements for August (in case of SA) and September. The large values of NMB for June 2005, and September 2005 and 2006 can be, at least partially, attributed to relatively small number of CL < 2 observations. The SA approach gives better results than CA only for July 2005, and June and July 2006.

At this stage of the research, mainly to the lack of data, the effect of cirrus clouds and LTF parameterization cannot be quantitatively addressed.

The main aim of this study is to apply the r.sun model to calculate the total radiation for clear sky conditions. Clear sky conditions (total cloudiness equal to 0) are, however, rare for the study area, and the question to answer is for which sky coverage (in octas) the clear sky model can give reasonable approximation of real solar radiation. Or, in other words, how the model error changes with increasing cloudiness? This issue is addressed in Fig. 7. Both CA and SA resulted in a small underestimation of CL = 0 conditions, with NMB and NMAE being closer to 0 for SA. For the CL < 3, the model can give quite accurate approximation of the real radiation flux, with the NMB below ±10% and NMAE not exceeding 0.3. The frequency of cloud conditions with CL < 3 exceeds 23%. For the CL > 2, the errors are at least doubled if compared with CL = 0 conditions.

The error assessment for various cloudiness conditions is based on the data collected on the PPS. It should be stressed here, that the cloudiness amount may change rapidly in space. This means that the uncertainties related with spatial modelling of clear sky solar radiation with the r.sun model may increase with distance from the PPS, for which information on CL are gathered. In future, this issue may be addressed with satellite-derived spatial information on cloudiness (Kotarba and Widawski 2008).

www.czasopisma.pan.pl PAN POLSKA AKADEMIA NAUK www.journals.pan.pl

Summary

The results of the r.sun model, applied here for the clear sky condition total (direct + diffuse) solar radiation calculation over the SW Spitsbergen area, have been found to be in good agreement with measurements collected at the PPS. The r.sun model can therefore be treated as a reliable and efficient tool providing detailed spatial and temporal patterns of incoming solar radiation for studies on various environmental phenomena, including glacier dynamics, hydrological studies *etc*. Although, the model tends to underestimate the solar total radiation, when compared with measurements. This can be attributed to misspecification of the Linke turbidity factor, simple temporal parameterization of AOT applied over the study period, and the definition of clear sky condition for model evaluation based only on low and middle level cloudiness data.

Linke turbidity factor was calculated with the formula proposed by Dogniaux (1984). The formula is widely used and was compared with the measurement-based LTF by Jacovides (1997), showing good agreement. However, the validation of the Dogniaux formula was performed for different climatological and astronomical (solar elevation) conditions (long term measurements obtained at Athens Observatory, presented by Jacovides 1997) and should be performed with the measurements from the study area, if the necessary data are available.

The relation between the model performance and the AOT is not clear. The authors expected increase of model errors for spring, when frequency of the Arctic haze phenomena is higher. This expectation is not confirmed by the results. The higher turbidity in spring is a physical fact, supported with significantly higher AOT values measured in April and May over the study period. Therefore, it is possible that the AOT-related error may be covered with, for example, miscalculation of the LTF. LTF calculation and verification, and AOT parameterization seem to be a key issue for the further improvements in model performance.

The model gives reasonable approximation of the solar radiation flux for the $CL < 3$ cloudiness conditions. The frequency of $CL < 3$ conditions for the study period was quite large, reaching 23%. However, the application of the r.sun model for the various cloudiness conditions is a task of great potential applicability which should be undertaken in the future. More complex approach to the parameterization of the role of aerosols on solar radiation should be applied, as this have large impact on the modelled spatial patterns of the solar radiation. Due to sparse measurements of the atmospheric aerosols over the Arctic areas, the other sources should also be considered, including air quality models.

Acknowledgements. — We gratefully acknowledge the reviewer, Dr Carleen Tijm-Reijmer (Utrecht University, Institute for Marine and Atmospheric Research) for the thorough review and comments, Institute of Geophysics (Polish Academy of Sciences) and University of Silesia for the measurement data and Digital Elevation Model used in this publication. The study was funded by the Ministry of Science and Higher Education grant no. 113/IPY/2007/01.

www.czasopisma.pan.pl PAN POLSKA AKADEMIA NAUK www.journals.pan.pl

References

DOGNIAUX R. 1984. De l'influence de l'estimation du facteur total de trouble atmosphérique sur l'évaluation du rayonnement solaire direct par ciel clair. Application aux données radiométriques de L'IRM à Uccle. in *Institut Royal Météorologique de Belgique (IRM), Miscellanea – Serie C* 20.

DUBAYAH R. and RICH P.M. 1995. Topographic solar radiation models for GIS. *International Journal of Geographical Information System* 9: 405–419. doi:10.1080/02693799508902046

FU P. and RICH P.M. 2000. The Solar Analyst 1.0 user manual. *Helios Environmental Modeling Institute* (http://www.hemisoft.com).

GRASS DEVELOPMENT TEAM 2006. www.grass.itc.it

HERBER A., THOMASON L. W., GERNANDT H., LEITERER U., NAGEL D., SCHULZ K.-H., KAPTUR J., ALBRECHT T. and NOTHOLT J. 2002. Continuous day and night aerosol optical depth observations in the Arctic between 1991 and 1999. *Journal of Geophysical Research* 107 (D10): 1–14. doi:10.1029/2001JD000536

HETRICK W.A., RICH P.M., BARNES F.J. and WEISS S.B. 1993. GIS-based solar radiation flux models. *American Society for Photogrammetry and Remote Sensing Technical papers. GIS, Photogrammetry and Modeling* 3: 132–143.

HOCK R. and HOLMGREN B. 2005. A distributed surface energy-balance model for complex topography and its application to Storglaciären, Sweden. *Journal of Glaciology* 51 (172): 25–36. doi:10.3189/172756505781829566

HODGKINS R. 2001. Seasonal evolution of meltwater generation, storage and discharge at non-temperate glacier in Svalbard. *Hydrological Processes* 15 (3): 441–460. doi:10.1002/hyp.160

HOFIERKA J. 1997. Direct solar radiation modelling within an open GIS environment. *Proceedings of the Joint European GI Conference 1997, Vienna*: 575–584.

HOFIERKA J. and ŠURI M. 2002. The solar radiation model for Open Source GIS: implementation and applications, *Proceedings of the Open Source GIS – GRASS users conference 2002 – Trento, Italy, 11–13 September 2002*.

JACOVIDES C.P. 1997. Model comparison for the calculation of the Linke's Turbidity Factor. *International Journal of Climatology* 17 (5): 551–563. doi:10.1002/(SICI)1097-0088(199704)17:5<551::AID-JOC137>3.0.CO;2-C

JANIA J. 1997. *Glaciology*. Wydawnictwo Naukowe PWN, Warszawa: 359 pp. (in Polish).

KLOK E.J. and OERLEMANS J. 2002. Model study of the spatial distribution of the energy and mass balance of Morteratschgletscher, Switzerland. *Journal of Glaciology* 48 (163): 505–518. doi: 10.3189/172756502781831133

KOTARBA A. and WIDAWSKI A. 2008. The satellite cloud climatology in 2007 above Svalbard in relation to atmospheric circulation conditions. *Problemy Klimatologii Polarnej* 18: 127–140 (in Polish).

KRZYŚCIN J.W. and SOBOLEWSKI P.S. 2001. The surface UV-B irradiation in the Arctic: observations at the Polish polar station, Hornsund (77°N, 15°E), 1996–1997. *Journal of Atmospheric and Solar-Terrestrial Physics* 63: 321–329. doi:10.1016/S1364-6826(00)00209-1

KUMAR L., SKIDMORE A.K. and KNOWLES E. 1997. Modelling topographic variation in solar radiation in a GIS environment. *International Journal of Geographic Information Science* 11 (5): 475–497. doi:10.1080/136588197242266

LOUCHE A., PERI G. and IQBAL M. 1986. An analysis of Linke Turbidity Factor. *Solar Energy* 6: 393–396. doi:10.1016/0038-092X(86)90028-9

LUND MYHRE C., TOLEDANO C., MYHRE G., STEBEL K., YTTRI K.E., AALTONEN V., JOHNSRUD M., FRIOUD M., CACHORRO V., de FRUTOS A., LIHAVAINEN H., CAMPBELL J.R., CHAIKOVSKY A.P., SHIOBARA M., WELTON E.J. and TORSETH K. 2007. Regional aerosol optical properties and radia-

www.czasopisma.pan.pl PAN POLSKA AKADEMIA NAUK www.journals.pan.pl

tive impact of the extreme smoke event in the European Arctic in spring 2006. *Atmospheric Chemistry and Physics* 7: 5899–5915.

MCKENNEY D.W., MACKEY B.G. and ZAVITZ B.L. 1999. Calibration and sensitivity analysis of a spatially-distributed solar radiation model. *International Journal of Geographic Information Science* 13 (1): 49–65. doi:10.1080/136588199241454

MIKLÁNEK P. 1993. The estimation of energy incoming grid points over the basin using simple digital elevation model. *Annales Geophysicae* (Supplement II) 11: 296.

PAGE J., ALBUISSON M. and WALD L. 2001. The European Solar Radiation Atlas: a valuable digital tool. *Solar Energy* 71: 81–83. doi:10.1016/S0038-092X(00)00157-2

POHL S., MARSH P. and PLETRONIRO A. 2006. Spatial-temporal variability in solar radiation during spring snowmelt. *Nordic Hydrology* 37 (1): 1–19.

SCHARMER K. and GREIF J. (eds) 2000. *The European Solar Radiation Atlas, Volume 2: Database and Exploitation Software*. Les Presses de l'École des Mines, Paris (http://www.helioclim.net/esra/index.html).

STOHL A., BERG T., BURKHART J.F., FJÆRAA A.M., FORSTER C., HERBER A., Hov Ø., LUNDER C., MCMILLAN W.W., OLTMANS S., SHIOBARA M., SIMPSON D., SOLBERG S., STEBEL K., STRÜOM J., TØRSETH K., TREFFEISEN R., VIRKKUNEN K. and YTTRI K.E. 2007. Arctic smoke – record high air pollution levels in the European Arctic due to agricultural fires in Eastern Europe in spring 2006. *Atmospheric Chemistry and Physics* 7: 511–534.

ŠURI M. and HOFIERKA J. 2004. A new GIS-based solar radiation model and its application to photovoltaic assessments. *Transactions in GIS* 8 (2): 175–190. doi:10.1111/j.1467-9671.2004.00174.x

TOLEDANO C., CACHORRO V., BERJÓN A., SORRIBAS M., VERGAZ R., DE FRUTOS A., ANTÓN M. and GAUSA M. 2006. Aerosol optical depth at ALOMAR Observatory (Andøya, Norway) in summer 2002 and 2003. *Tellus* 58B: 218–228.

UTRILLAS M.P., PEDROS R., MARTINEZ-LOZANO J.A. and TENA F. 2000. A new method for determining the Angström turbidity coefficient from broadband filter measurements. *Journal of Applied Meteorology* 39: 863–874. doi:10.1175/1520-0450(2000)039<0863:ANMFDT>2.0.CO;2

VAN DE WAL R.S.W., BOOT W., VAN DEN BROEKE M.R., SMEETS C.J.P.P., REIJMER C.H., DONKER J.J.A. and OERLEMANS J. 2008. Large and rapid velocity changes in the ablation zone of the Greenland ice sheet. *Science* 321: 111–113. doi:10.1126/science.1158540 PMid:18599784

VIDA J., FOYO-MORENO I. and ALADOS-ARBOLEDAS L. 1999. Performance validation of MURAC, a cloudless sky radiance model proposal. *Energy* 24: 705–721. doi:10.1016/S0360-5442(99)00026-2

VIELI A., JANIA J., BLATTER H. and FUNK M. 2004. Short-term velocity variations on Hansbreen, a tidewater glacier in Spitsbergen. *Journal of Glaciology* 50: 389–398. doi:10.3189/172756504781829963

YAMANOUCHI T., TREFFEISEN R., HERBER A., SHIOBARA M., YAMAGATA S., HARA K., SATO K., YABUKI M., TOMIKAWA Y., RINKE A., NEUBER R., SCHUMACHTER R., KRIEWS M., STROEM J., SCHREMS O. and GERNANDT H. 2005. Arctic study of tropospheric aerosol and radiation (ASTAR) 2000: Arctic haze case study. *Tellus* 57B: 141–152.

YU S., EDER B., DENNIS R., CHU S. and SCHWARTZ S.E. 2006. An unbiased symmetric metrics for evaluation of air quality models. *Atmospheric Science Letters* 7: 26–34. doi:10.1002/asl.125

ZWALLY H.J., ABDALATI W., HERRING T., LARSON K., SABA J. and STEFFEN K. 2002. Surface Melt-Induced Acceleration of Greenland Ice-Sheet Flow. *Science* 297: 218–222. doi:10.1126/science.1072708 PMid:12052902

Received 17 February 2009
Accepted 10 December 2009